ACS APPLIED MATERIALS & INTERFACES

Forum Article

www.acsami.org

Effect of Lanthanide Metal Complexation on the Properties and Electronic Structure of Single-Walled Carbon Nanotube Films

Matthew L. Moser,[†,‡] Aron Pekker,[†,‡] Xiaojuan Tian,[‡,§] Elena Bekyarova,[†,‡] Mikhail E Itkis,[†,‡] and Robert C Haddon*[,†,§]

[†]Department of Chemistry, [‡]Center for Nanoscale Science and Engineering, and [§]Department of Chemical Engineering, University of California, Riverside, California 92521, United States

ABSTRACT: We spectroscopically analyze the effect of e-beam deposition of lanthanide metals on the electronic structure and conductivities of films of semiconducting (SC) single-walled carbon nanotubes (SWNTs) in high vacuum. We employ near-infrared and Raman spectroscopy to interpret the changes in the electronic structure of SWNTs on exposure to small amounts of the lanthanides (Ln = Sm, Eu, Gd, Dy, Ho, Yb), based on the behavior of the reference metals (M = Li, Cr) which are taken to exemplify ionic and covalent bonding, respectively. The analysis shows that while the lanthanides are more electropositive than the transition metals, in most cases they exhibit similar conductivity behavior which we interpret in terms of the formation of covalent bis-hexahapto bonds [(η^6-SWNT)M(η^6-SWNT), where M = La, Nd, Gd, Dy, Ho]. However, only M = Eu, Sm, Yb show the continually increasing conductivity characteristic of Li, and this supports our contention that these metals provide the first examples of mixed covalent−ionic bis-hexahapto bonds [(η^6-SWNT)M(η^6-SWNT), where M = Sm, Eu, Yb].

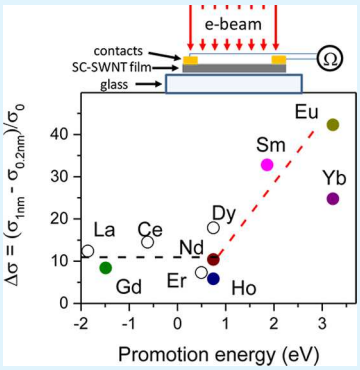

KEYWORDS: *carbon nanotube film, lanthanides, organometallic, conductivity, optical properties*

INTRODUCTION

The diversity of electronic structures available in organometallic complexes of the lanthanides has undergone a dramatic revision over the last 40 years. The organometallic complexes of the lanthanides were originally confined to the +3 oxidation state and the field was dominated by studies of the π-bonded tricyclopentadienyls [Ln(η^5-C_5H_5)$_3$], which are often associated in the solid state due to the their unsaturated coordination.[1] However, organometallic complexes of the +2 oxidation state followed and have been extended to all of the lanthanide elements[2] and zerovalent lanthanide organometallics have been characterized in which substituted benzene molecules function as the π-bonded ligand [Ln(η^6-^{t}Bu$_3$C$_6$H$_3$)$_2$].[3]

We have used this latter bonding motif to augment our use of the transition metal chemistry of the graphene surfaces of carbon nanomaterials,[4,5] to enhance the conductivity of single-walled carbon nanotube (SWNT) networks by e-beam deposition of selected lanthanide atoms, Ln = La, Nd, Sm, Eu, Gd.[6] Prior to this work, the deposition of chromium had led to the largest enhancement in the conductivity of SWNT networks, exceeding the values obtained with M = Ti, V, Mn, Fe,[7] and M = Mo, W.[8] However, when we examined the lanthanide data we found that there were two different behaviors: those which gave conductivity enhancements less than Cr and fairly typical of other transition metals examined to date (Ln = La, Nd, Gd), and those that exceeded the Cr values (Ln = Sm, Eu).[6] We were able to rationalize the conductivity data by reference to a model which is based on the accessibility of the 4f^m 5d^1 6s^2 electronic configuration for the individual lanthanide atoms.[3,9] In applying this model we suggested that the elements Sm and Eu were able to strongly enhance the conductivity of the SWNT films due to the ability of these metals to not only engage in bis-hexahapto-bonding [which is the characteristic feature of all of these (η^6-SWNT)M(η^6-SWNT) organometallic complexes], but to also transfer charge into the conduction band of the SWNTs due to the symmetry of the frontier molecular orbitals (FMOs) in the lanthanide complexes, and the fact that the partially filled metal 5d orbitals involved in the interaction lie relatively high in energy in the case of Sm and Eu.[6]

Although the original work on the lanthanide complexes of benzene [Ln(η^6-^{t}Bu$_3$C$_6$H$_3$)$_2$] confirmed the formulation of these compounds as neutral, covalent, π-bonded molecules in which the metal was zerovalent,[3] the lanthanide compounds of C_{60} began with the idea that they would form salts[10] in analogy with the ionic alkali metal fullerides.[11,12] Indeed, the observation that some of these compounds (M = Yb, Sm) are superconductors strongly supports the idea that there are free electrons in these compounds which reside primarily on C_{60},[10,13,14] as do the physical properties of the Eu$_x$C$_{60}$ compounds.[15] All of these authors assign the oxidation state of the lanthanide as +2 but the importance of covalent

Special Issue: Advances towards Electronic Applications in Organic Materials

Received: January 31, 2015
Accepted: April 9, 2015
Published: April 23, 2015

DOI: 10.1021/acsami.5b00942
ACS Appl. Mater. Interfaces 2015, 7, 28013−28018

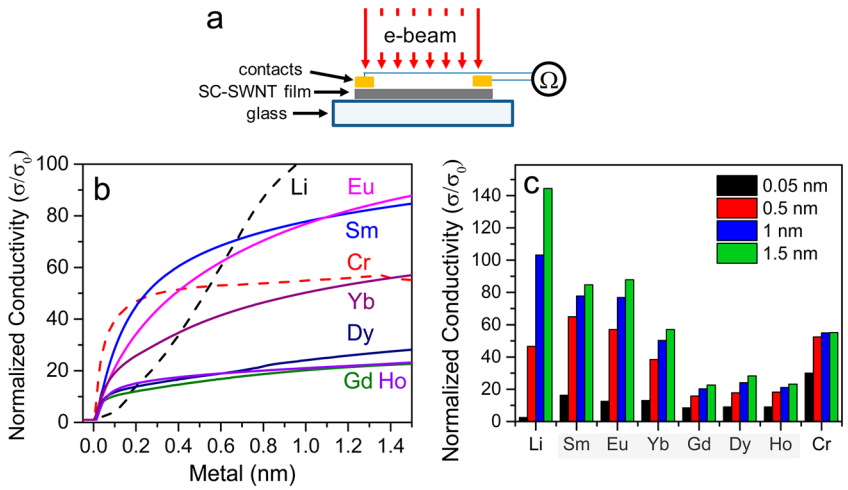

Figure 1. Effect of metal deposition on electrical conductivity of SC-SWNT films: (a) Schematic illustration of the experimental configuration of the in situ measurements of the film resistance during e-beam metal evaporation. (b) Change of SC-SWNT film conductivity as a function of deposited metal thickness; the values are normalized to the conductivity of pristine SC-SWNT film. (c) Normalized conductivities of SC-SWNT films with deposited metal of thicknesses 0.05, 0.5, 1, and 1.5 nm.

character in these compounds is discussed at length.[14,15] In this respect, the C_{60} compounds are rather different from the lanthanide complexes of benzene and SWNTs discussed above in that C_{60} is strongly curved and possesses five-membered rings (5-MRs); these features of the geometric and electronic structure contribute to the ability of the fullerenes to stabilize excess electron density.[16,17] Although the fullerenes are incapable of forming stable π-complexes with transition metals requiring a hapticity greater than two, given the size and orbital extent of the lanthanides, they may be effective in facilitating η^5-coordination of the 5-MRs.[14,18] Nevertheless, it is apparent that similar issues are relevant in the C_{60} and SWNT complexes of the lanthanides; that is, the question of covalent and ionic bonding, although the fullerides prepared to date only include M = Sm, Eu, and Yb, which are known to readily form the +2 oxidation state.[3]

As noted above, we assigned a mixed [bis(hexahapto)] covalent, ionic structure to the compounds formed on interaction of the metals M = Sm, Eu with SWNT films on the basis of their strongly enhanced conductivities.[6] Given the importance of this question, we wanted to substantiate this suggestion with direct measurements of the charge density distributions in the (η^6-SWNT)M(η^6-SWNT) compounds, where M = Ln. Recently, we showed that both near-IR and Raman spectroscopy were able to provide such information in studies on SWNT films subjected to treatment with M = Au (physisorption), Li (chemisorption with ionic doping) and Cr (chemisorption with covalent hexahapto-bonding).[19] In the present paper we apply these techniques to SWNT films which have been subjected to high vacuum e-beam lanthanide deposition as well as extending our studies to include additional lanthanides, M = Dy, Ho, Yb. We are able to confirm our previous assignments regarding the lanthanide charge density distributions and we show that this series of metals functions as both neutral bis(hexahapto) π-complexes [analogous to the Ln(η^6-^{t}Bu$_3$C$_6$H$_3$)$_2$ compounds], but also as bis(hexahapto) π-complexes in which there is charge transfer to the conduction band of the SWNT backbone that further enhances the conductivity—in analogy with the M_xC_{60} compounds where M = Sm, Eu, Yb,[10,13−15] (discussed in detail below).

RESULTS

Electrical Conductivity. The metal deposition experiments were performed on films of semiconducting (SC−) SWNTs (thickness, t = 8 nm), which were mounted on substrates with gold contacts and transferred to a cryo-pumped Temescal BJD 1800 e-beam evaporator equipped with custom fittings to allow the measurement of the in situ film resistance (Figure 1a);[7,20] the initial resistance of the films was R = 1 MΩ (σ = 2 S/cm). In addition to the lanthanides, two other metals were included for comparison purposes: Cr, which forms a covalent hexahapto-bond to the SWNTs[7,19,21−26] and Li, which exhibits ionic doping of the SWNTs. The changes in the SWNT film conductivity on deposition of various metals are collected in Figure 1b and discussed in detail later in the paper. Briefly, charge transfer is exemplified by Li, which induces a linear enhancement of the SWNT film conductivity and produces a 100 fold increase in conductivity at metal thickness t = 1 nm, whereas chromium shows an abrupt increase of conductivity which saturates beyond t = 0.2 nm. As noted previously,[6] in the initial stages of the deposition of the lanthanide metals (below 0.1 nm), there is a sharp increase in the SWNT conductivity which resembles the behavior of Cr. However, beyond this initial increase, the lanthanides exhibit two divergent behaviors in their effect on the SWNT conductivities: the enhancements produced by Dy, Ho, and Gd are quite modest and show saturation, whereas Sm, Eu, and Yb have a more pronounced effect.

Figure 1c compares the conductivity increase due to the deposition of Li, Cr and the lanthanides. The data are normalized to the conductivity of the SC-SWNT films prior to deposition. It is apparent that at very low metal coverage (t = 0.05 nm) the effect of Li is very small, whereas Cr increases the film conductivity by more than 30 times and the lanthanides fall between these two extreme cases giving conductivity enhancements of ∼10.

Spectroscopy. To spectroscopically characterize the effect of metal deposition on the SWNT samples it was necessary to remove the substrates from the e-beam apparatus and because of the sensitivity of the materials to the atmosphere, the samples were coated with aluminum before exposure to the atmosphere. Thus, for the spectroscopic experiments, the

DOI: 10.1021/acsami.5b00942
ACS Appl. Mater. Interfaces 2015, 7, 28013−28018

SWNT films were mounted on thin borosilicate glass slides and 2.5 nm of the subject metal was deposited by e-beam evaporation (Li, Cr, Sm, Eu, Gd, Dy, Ho, or Yb), followed by an aluminum protective layer (50 nm). The optical measurements were performed in reflection mode through the thin borosilicate glass backside of the samples (Figure 2a).

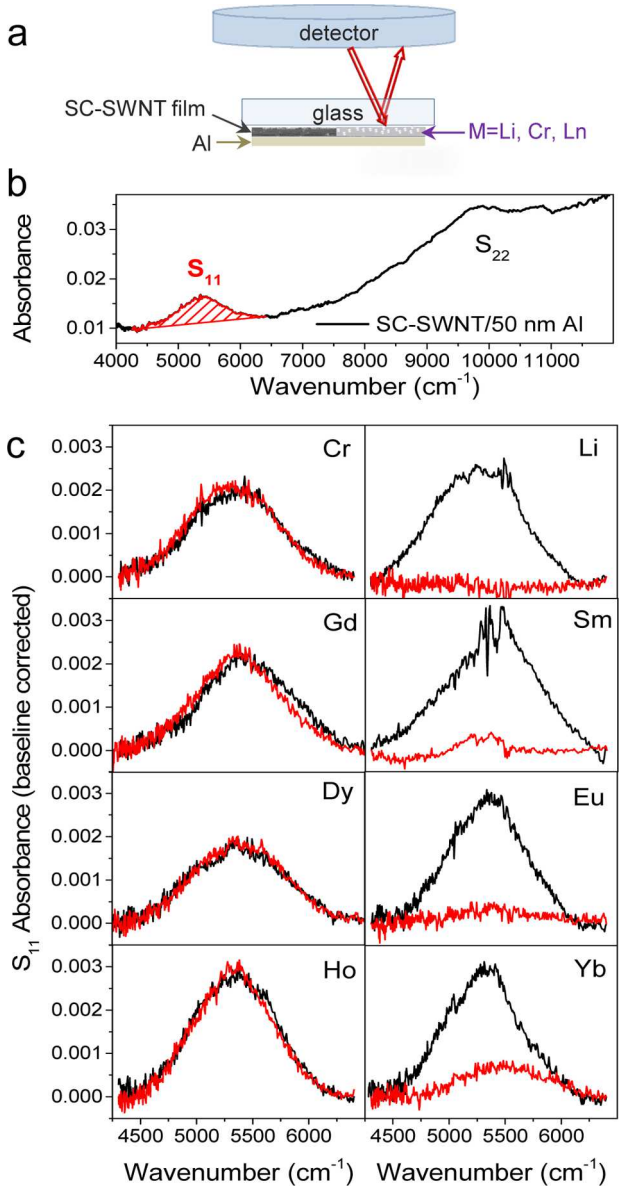

Figure 2. Absorption spectroscopy of SWNT films as a function of metal deposition. (a) Schematics of sample configuration and measurement setup. (b) Spectrum of a SWNT sample covered with 50 nm aluminum layer. Dashed line illustrates the S_{11} region and the linear baseline correction. (c) S_{11} interband transition of the nanotube films after baseline correction: reference (black, without metal) and sample (red, with deposited metal) (see text).

Figure 2b displays a typical spectrum of the SC-SWNTs; the arc-discharge semiconducting SWNTs have an average diameter of 1.5 nm and their interband electronic transitions occur at ~0.6 eV (S_{11}) and ~1.1 eV (S_{22}). The intensities of these transitions are sensitive to the position of the Fermi level and electron donation shifts the Fermi level into the van Hove singularities, which suppresses the interband transitions due to Pauli blocking, resulting in reduced peak intensities.[27−29] Thus, the intensities of the interband electronic transitions provide a sensitive indicator of the charge density on the SWNTs and in order to evaluate the electronic character of the interaction of the lanthanide metals with the SWNTs we studied the intensities of the S_{11} transitions of the SWNT films.

Figure 2c illustrates the baseline corrected spectra and in each experiment the spectrum of SC-SWNTs with deposited metal (2.5 nm) is compared with that of pristine SC-SWNTs collected from the same film. For comparison purposes the metal was deposited on one-half of the SWNT film, while the other half was protected from metal deposition by placement of a custom-made shutter in the path of the metal flux. Following the deposition of the subject metal, the shutter was moved aside to allow the deposition of a 50 nm protective aluminum coating which covered the whole SWNT film, thereby allowing the simultaneous preparation of a sample with a metal-SWNT region and a pristine SWNT reference region in order to allow a direct comparison of the effect of the metal on the sample under study.

In agreement with our previous experiments, chromium deposition exerted little or no effect on the intensity of the S_{11} peak,[8,19] and the same was true of the lanthanides Ln = Gd, Dy, and Ho, thus suggesting that the enhancement in conductivity brought about by these metals is due almost entirely to metal hexahapto-bond formation.[6] Deposition of lithium completely suppressed the S_{11} transition, in accordance with its strongly electron donating nature. Similarly, the optical measurements showed that Sm and Eu almost completely suppress the S_{11} peak, whereas in the case of ytterbium, there is still a detectable S_{11} peak, suggesting a slightly weaker doping effect.

Raman Spectroscopy. The Raman spectrum of SWNTs is also sensitive to the charge density and Figure 3a gives a typical Raman spectrum of a SC-SWNT film; the spectrum displays four main features:[30] a G-peak - characteristic of all sp^2 hybridized carbon networks and associated with the Γ-point phonon mode; a small D-peak (disorder), associated with a K-point phonon mode which is activated by inelastic scattering of electrons on imperfections in the lattice such as defects, edges or grain boundaries; a radial-breathing mode (RBM) peak, related to the diameter of the nanotubes; and a 2D-peak, which is an overtone of the D-peak but its activation does not involve the presence of defects. In the presence of doping some of the associated phonon mode frequencies are renormalized due to electon-phonon coupling, resulting in a shift in the peak position.[31−33] For the purposes of our experiments we focused on the effect of metal deposition on the 2D peak of the SWNT films. The 2D peak position in semiconducting SWNTs is downshifted by electron doping,[32] and this effect can be utilized to elucidate the extent of charge transfer between the active metal and the SWNTs.

The samples for the Raman experiments were prepared in the same way as for the absorption measurements (Figure 2a). Figure 3b shows a comparison of the spectra of selected samples; black curves represent the reference SC-SWNT region, whereas red curves show the Raman spectrum of the region with deposited active metal. Multiple spots were measured on each sample and the mean values are compared in Figure 3c. Li, Sm, and Eu induce a large downshift corresponding to significant electron donation from the metal to the nanotube, whereas Yb only moderately shifts the 2D peak position of the SC-SWNTs. Cr, Al, Gd, Dy, and Ho show

DOI: 10.1021/acsami.5b00942
ACS Appl. Mater. Interfaces 2015, 7, 28013−28018

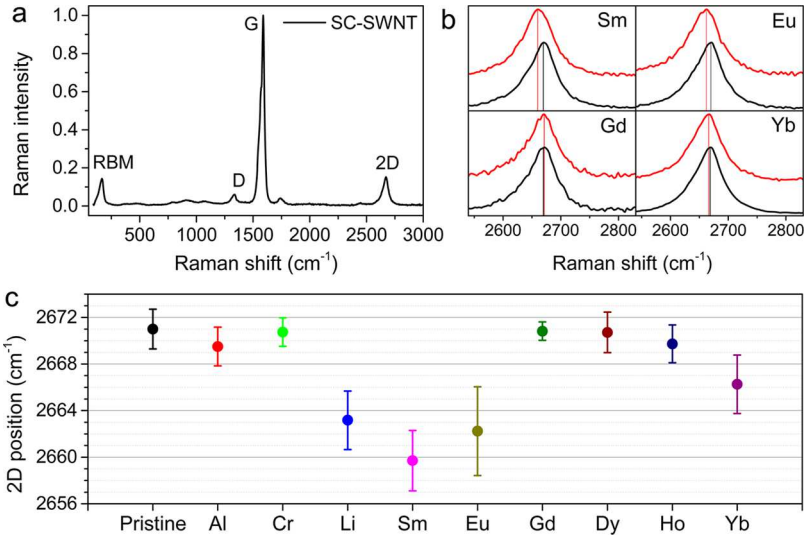

Figure 3. Raman spectroscopy of SWNT films as a function of metal deposition. (a) Raman spectrum of a SC-SWNT film. The four most prominent features are labeled: RBM, radial breathing mode, D, disorder peak, G, graphitic peak, 2D peak, peak overtone of the D peak. (b) 2D region of the Raman spectra of selected samples of SWNT films with deposited metal (M = Sm, Eu, Gd, and Yb) (red) and reference spectra (black, pristine SC-SWNT) (see text). (c) Mean and standard deviation of 2D peak positions of the samples.

little or no effect on the peak position, indicating the absence of ionic character in their interaction with the SWNTs.

DISCUSSION

The standard model of bis-hexahapto-lanthanide complexation requires the participation of the $4f^m$ $5d^1$ $6s^2$ lanthanide electronic configuration,[3,9,34] and this mode of bonding operates with a 15 electron valence shell electronic structure. According to this model the stability of the bis-hexahapto-lanthanide complexes depends on the accessibility of the $5d^1$ $6s^2$ electronic structure and we have previously shown that such an analysis accounts for the variations in the conductivity enhancements measured for the series, Ln = La, Nd, Sm, Eu, Gd.[6] In this analysis, we suggested that the additional enhancement in the conductivities induced by Eu and Sm relative to the other lanthanides (La, Nd, Gd) was due to the ability of Eu and Sm to transfer electron density to the SWNT conduction band via the bis-hexahapto-bonds at the SWNT junctions.[6] Thus, it was of interest to explore the relationship of the Raman 2D peak shift because of electron density donation to the SWNTs (Figure 4a) with the promotion energy necessary to achieve the $4f^m$ $5d^1$ $6s^2$ lanthanide electronic configuration and it may be seen in Figure 4a that the Raman data suggest that Eu, Sm and Yb are able to transfer electrons to the SWNT conduction band.

Although all of the metals enhance the SWNT film conductivities, there are distinct differences in the character of the conductivity response (Figure 1): the transition metals and lanthanides are characterized by an abrupt change in conductivity at low coverage ($t \leq 0.2$ nm), whereas simple doping (Li), shows a more gradual, continuous increase in the film conductivity which we have attributed to the transfer of electrons to the SWNT conduction band.[4,7] Furthermore, in our studies of the effect of Au, Li and Cr on the percolation threshold of very thin SWNT films it was apparent that the ability of Cr to form bis-hexahapto bonds and thereby bridge SWNT junctions was most apparent at low metal coverage because of the very small number of sites with the geometry necessary for this reaction.[19] To capture the distinction

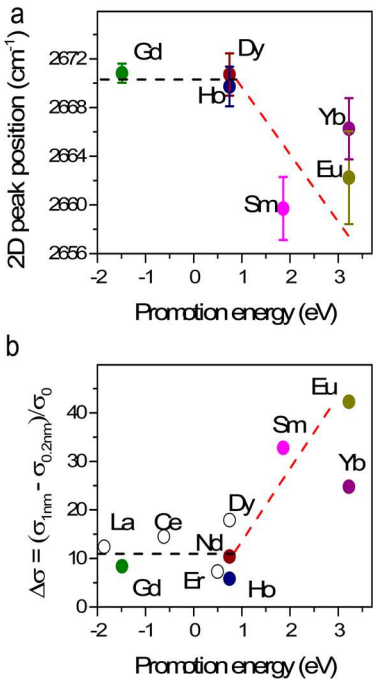

Figure 4. Relationship of the lanthanide promotion energies (see text), to the Raman shifts and conductivities of the SWNT networks after lanthanide deposition. (a) Promotion energy as a function of the Raman 2D peak position. (b) Promotion energy as a function of the differential conductivity enhancement, $\Delta\sigma = (\sigma_{1\text{ nm}} - \sigma_{0.2\text{ nm}})/\sigma_0$. Dashed lines are guides to the eye.

between these two modes of metal−SWNT interactions, we introduce the differential conductivity enhancement ($\Delta\sigma$), which in the present context we define as $\Delta\sigma = [\sigma_{(t=1.0\text{ nm, metal})} - \sigma_{(t=0.2\text{ nm, metal})}]/\sigma_o$ (where σ_o is the conductivity of the pristine SWNT film), with the goal of defining an index of covalent and ionic character in metal-SWNT bonding. On the basis of the previous discussion, this parameter should be directly related to the promotion energy necessary to achieve the $4f^m$ $5d^1$ $6s^2$ lanthanide electronic configuration (as shown in

DOI: 10.1021/acsami.5b00942
ACS Appl. Mater. Interfaces 2015, 7, 28013−28018

Figure 4b), because this latter quantity determines the relative placement of the lanthanide d-orbitals and the SC-SWNT conduction band.[6]

CONCLUSION

The differential conductivity ($\Delta\sigma$), which provides a measure of the conductivity enhancement as a function of coverage, reflects the contribution of ionic character in the (η^6-SWNT)Ln(η^6-SWNT) hexa-hapto bonds. Low values of $\Delta\sigma$ imply purely covalent bonding (La, Nd, Gd, Dy, Ho), whereas an increase in $\Delta\sigma$ is associated with the involvement of charge transfer to the SWNT conduction band in addition to hexa-hapto bond formation (Eu, Sm, Yb). As expected, $\Delta\sigma$ is related to the promotion energy necessary to achieve the $4f^m$ $5d^1$ $6s^2$ lanthanide electronic configuration (Figure 4b), because this latter quantity dictates the energetics of the charge transfer process.[6] Thus, we conclude that all of the lanthanides exhibit the initial abrupt increase in conductivity at low coverage, which is characteristic of the transition metals, but only Eu, Sm, Yb show the continually increasing conductivity characteristic of strong electron donors (Figures 1 and 4b, large values of $\Delta\sigma$), and this supports our contention that these latter metals provide the first examples of mixed covalent−ionic bis-hexahapto bonds [(η^6-SWNT)M(η^6-SWNT), where M = Sm, Eu, Yb].[6]

The ability to modify and interconnect the electronic structures of graphitic surfaces by single atom covalent and ionic bonding (atomtronics),[5] suggests the application of this approach in catalysis, high mobility transistor, spintronic and memory devices.[22,35,36] Furthermore, there is the promise of new ferromagnetic and superconducting materials based on the organometallic single layer graphene and graphene sandwich compounds and their relationship to the graphite and C_{60} intercalation compounds.[4,5,10,12−15,21,35,37]

METHODS

The experiments made use of electric arc separated semiconducting SWNTs obtained from NanoIntegris Inc. (IsoNanotubes, 99%), with average diameter and length of 1.2−1.7 nm and 300 nm to 2 μm, respectively.

The in situ conductivity measurements were performed with 8 nm thick SC-SWNT films prepared on alumina membranes via vacuum filtration. Film thickness was determined using SWNT density of 1.2 g/cm^3.[38] One milliliter of SWNT solution (0.01 mg/mL) was mixed with 50 mL of DI water, then vacuum filtered onto the alumina membrane (Anodisc 47, 47 mm diameter, 0.02 μm) and was washed with a mixture of DI water and ethanol to remove remaining surfactant residues on the film. The alumina membranes were cut into 4 mm × 3 mm rectangles, positioned onto prepatterned gold electrodes, and contacted with conductive silver paste. The films were annealed at 300 °C for 3 h in vacuum (1×10^{-7} Torr) to remove contaminants. The SC-SWNT films showed initial conductivities of σ = 2 S/cm.

Near-IR (NIR) and Raman spectroscopic studies were performed on 4 nm-thick SC-SWNT films prepared by vacuum filtration on nitrocellulose membranes (Millipore, 0.1 μm VCWP). These samples were made by first placing a small piece of SC-SWNT film on a nitrocellulose membrane in contact with a thin borosilicate glass slide. Then the filter membrane was removed in a bath of acetone vapors over a period of 1 h. The films were then annealed using the same conditions described above.

Li, Cr, Sm, Eu, Dy, Ho, Yb, and Al deposition sources were obtained from Kurt Lesker. The in situ conductivity measurements were carried out in a modified Temescal BJD 1800 e-beam evaporator and used a Kiethley 2700 to measure the two point resistance of the samples. All films were exposed to the metal vapor at a deposition rate of 0.3−0.5 Å per second at a chamber pressure of $2-5 \times 10^{-6}$ Torr. For the optical spectroscopy, 2.5 nm of the metal of interest was allowed to deposit on half of the film. A homemade in-chamber shutter protected the other half from exposure to metal vapor and could be mechanically removed while keeping the chamber in high vacuum conditions. Once the shutter was removed, 50 nm of the covering metal (aluminum) was deposited. This gave each sample two distinct regions for characterization; a reference SC-SWNT film and a SC-SWNT film area which was exposed to the metal flux. The encapsulating Al layer allowed sample manipulation in the atmosphere without degradation of the metal-SWNT films.

Near-infrared spectra were taken with a Jobin-Yvon iHR 320 spectrometer in combination with a Bruker Hyperion 1000 microscope and a MCT detector. Raman spectra were collected on a Nicolet Almega XS Raman spectrometer with 532 nm laser excitation and a laser power not exceeding 10%. To perform the measurements, we inverted the sample substrate, protected with an Al layer, and the spectra were taken through the glass slide. In the optical absorption measurements, the near-infrared radiation passed through the SWNT layer twice by reflection from the protective aluminum layer.

AUTHOR INFORMATION

Corresponding Author

*E-mail: haddon@ucr.edu.

Notes

The authors declare no competing financial interest.

ACKNOWLEDGMENTS

The study was supported by NSF under contract DMR-1305724. M.L.M. acknowledges support through the U.S. Department of Education GAANN award P200A120170.

REFERENCES

(1) Schumann, H. Organolanthanoid Compounds. *Angew. Chem., Int. Ed.* **1984**, *23*, 474−493.

(2) MacDonald, M. R.; Bates, J. E.; Ziller, J. W.; Furche, F.; Evans, W. J. Completing the Series of +2 Ions for the Lanthanide Elements: Synthesis of Molecular Complexes of Pr^{2+}, Gd^{2+}, Tb^{2+}, and Lu^{2+}. *J. Am. Chem. Soc.* **2013**, *135*, 9857−9868.

(3) Cloke, F. G. N. Zero Oxidation State Compounds of Scandium, Yttrium, and the Lanthanides. *Chem. Soc. Rev.* **1993**, 17−24.

(4) Bekyarova, E.; Sarkar, S.; Wang, F.; Itkis, M. E.; Kalinina, I.; Tian, X.; Haddon, R. C. Effect of Covalent Chemistry on the Electronic Structure and Properties of Carbon Nanotubes and Graphene. *Acc. Chem. Res.* **2013**, *46*, 65−76.

(5) Sarkar, S.; Moser, M. L.; Tian, X.; Zhang, X. J.; Al-Hadeethi, Y. F.; Haddon, R. C. Metals on Graphene and Carbon Nanotube Surfaces: From Mobile Atoms to Atomtronics to Bulk Metals to Clusters and Catalysts. *Chem. Mater.* **2014**, *26*, 184−195.

(6) Moser, M. L.; Tian, X.; Pekker, A.; Sarkar, S.; Bekyarova, E.; Itkis, M. E.; Haddon, R. C. Hexahapto-Lanthanide Interconnects Between the Conjugated Surfaces of Single-Walled Carbon Nanotubes. *Dalton Trans.* **2014**, *43*, 7379−7382.

(7) Wang, F.; Itkis, M. E.; Bekyarova, E.; Tian, X.; Sarkar, S.; Pekker, A.; Kalinina, I.; Moser, M.; Haddon, R. C. Effect of First Row Transition Metals on the Conductivity of Semiconducting Single-Walled Carbon Nanotube Networks. *Appl. Phys. Lett.* **2012**, *100*, 223111.

(8) Kalinina, I.; Bekyarova, E.; Sarkar, S.; Wang, F.; Itkis, M. E.; Tian, X.; Niyogi, S.; Jha, N.; Haddon, R. C. Hexahapto-Metal Complexes of Single-Walled Carbon Nanotubes. *Macromol. Chem. Phys.* **2012**, *213*, 1001−1019.

(9) Anderson, D. M.; Cloke, F. G. N.; Cox, P. A.; Edelstein, N.; Green, J. C.; Pang, T.; Sameh, A. A.; Shalimoff, G. On the Stability and Bonding in bis(η-arene) Lanthanide Complexes. *J. Chem. Soc., Chem. Commun.* **1989**, 53−55.

DOI: 10.1021/acsami.5b00942
ACS Appl. Mater. Interfaces 2015, 7, 28013−28018

(10) Ozdas, E.; Kortan, A. R.; Kopylov, N.; Ramirez, A. P.; Siegrist, T.; Rabe, K. M.; Bair, H. E.; Schuppler, S.; Citrin, P. H. Superconductivity and Cation-Vacancy Ordering in the Rare-earth Fulleride $Yb_{2.75}C_{60}$. *Nature* **1995**, *375*, 126−129.
(11) Haddon, R. C.; Hebard, A. F.; Rosseinsky, M. J.; Murphy, D. W.; Duclos, S. J.; Lyons, K. B.; Miller, B.; Rosamilia, J. M.; Fleming, R. M.; Kortan, A. R.; Glarum, S. H.; Makhija, A. V.; Muller, A. J.; Eick, R. H.; Zahurak, S. M.; Tycko, R.; Dabbagh, G.; Thiel, F. A. Conducting Films of C_{60} and C_{70} by Alkali Metal Doping. *Nature* **1991**, *350*, 320−322.
(12) Haddon, R. C. Electronic Structure, Conductivity and Superconductivity in Alkali Metal Doped C_{60}. *Acc. Chem. Res.* **1992**, *25*, 127−133.
(13) Chen, X. H.; Roth, G. Superconductivity at 8K in Samarium-Doped C_{60}. *Phys. Rev. B* **1995**, *52*, 15534−15536.
(14) Citrin, P. H.; Ozdas, E.; Schuppler, S.; Kortan, A. R.; Lyons, K. B. Distorted and Inequivalently Charged C_{60} Anions in $Yb_{2.75}C60$. *Phys. Rev. B* **1997**, *56*, 5213−5227.
(15) Ginwalla, A. S.; Balch, A. L.; Kauzlarich, S. M.; Irons, S. H.; Klavins, P.; Shelton, R. N. Synthesis and Characterization of the Europium Fullerides Eu_xC60 (x = 1−6). *Chem. Mater.* **1997**, *9*, 278−284.
(16) Haddon, R. C.; Brus, L. E.; Raghavachari, K. Electronic Structure and Bonding in Icosahedral C_{60}. *Chem. Phys. Lett.* **1986**, *125*, 459−464.
(17) Haddon, R. C. The Fullerenes: Powerful Carbon-Based Electron Acceptors. *Philos. Trans. R. Soc., A* **1993**, *343*, 53−62.
(18) Haddon, R. C. Organometallic Chemistry of the Fullerenes: η^2- and η^5-(π) Complexes. *J. Comput. Chem.* **1998**, *19*, 139−143.
(19) Tian, X.; Moser, M. L.; Pekker, A.; Sarkar, S.; Ramirez, J.; Bekyarova, E.; Itkis, M. E.; Haddon, R. C. Effect of Atomic Interconnects on Percolation in Single-Walled Carbon Nanotube Thin Film Networks. *Nano Lett.* **2014**, *14*, 3930−3937.
(20) Wang, F.; Itkis, M. E.; Bekyarova, E.; Sarkar, S.; Tian, X.; Haddon, R. C. Solid-state Bis-hexahapto Metal Complexation of Single-Walled Carbon Nanotubes. *J. Phys. Org. Chem.* **2012**, *25*, 607−610.
(21) Tian, X.; Sarkar, S.; Moser, M. L.; Wang, F.; Pekker, A.; Bekyarova, E.; Itkis, M. E.; Haddon, R. C. Effect of Group 6 Transition Metal Coordination on the Conductivity of Graphite Nanoplatelets. *Mater. Lett.* **2012**, *80*, 171−174.
(22) Avdoshenko, S. M.; Ioffe, I. N.; Cuniberti, G.; Dunsch, L.; Popov, A. A. Organometallic Complexes of Graphene: Toward Atomic Spintronics using a Graphene Web. *ACS Nano* **2011**, *5*, 9939−9949.
(23) Li, E. Y.; Marzari, N. Improving the Electrical Conductivity of Carbon Nanotube Networks: A First-Principles Study. *ACS Nano* **2011**, *5*, 9726−9736.
(24) Dai, J.; Zhao, Y.; Wu, X.; Zeng, X. C.; Yang, J. Organometallic Hexahapto-Functionalized Graphene: Band Gap Engineering with Minute Distortion to the Planar Structure. *J. Phys. Chem. C* **2013**, *117*, 22156−22161.
(25) Ketolainen, T.; Havu, V.; Puska, M. J. Enhancing Conductivity of Metallic Carbon Nanotube Networks by Transition Metal Adsorption. *J. Chem. Phys.* **2015**, *142*, 054705.
(26) Gloriozov, I. P.; Marchal, R.; Saillard, J.-Y.; Oprunenko, Y. F. Chromium Tricarbonyl and Chromium Benzene Complexes of Graphene, their Properties, Stabilities, and Inter-ring Haptotropic Rearrangements - a DFT Investigation. *Eur. J. Inorg. Chem.* **2015**, *2015*, 250−257.
(27) Itkis, M. E.; Niyogi, S.; Meng, M.; Hamon, M.; Hu, H.; Haddon, R. C. Spectroscopic Study of the Fermi Level Electronic Structure of Single Walled Carbon Nanotubes. *Nano Lett.* **2002**, *2*, 155−159.
(28) Pichler, T.; Liu, X.; Knupfer, M.; Fink, J. Electronic Properties of Intercalated Single-Wall Carbon Nanotubes and C_{60} Peapods. *New J. Phys.* **2003**, *5*, 156.
(29) Wu, Z.; Chen, Z.; Du, X.; Logan, J. M.; Sippel, J.; Nikolou, M.; Kamaras, K.; Reynolds, J. R.; Tanner, D. B.; Hebard, A. F.; Rinzler, A. G. Transparent, Conductive Carbon Nanotube Films. *Science* **2004**, *305*, 1273−1276.
(30) Dresselhaus, M. S.; Saito, R.; Hofmann, M.; Dresselhaus, G.; Jorio, A. Raman Spectroscopy of Graphene and Carbon Nanotubes. *Adv. Phys.* **2011**, *60*, 413−550.
(31) Tsang, J. C.; Freitag, M.; Perebeinos, V.; Liu, J.; Avouris, Ph. Doping and Phonon Renormalization in Carbon Nanotubes. *Nat. Nanotechnol.* **2007**, *2*, 725−730.
(32) Das, A.; Sood, A. K. Renormalization of the Phonon Spectrum in Semiconducting Single-Walled Carbon Nanotubes Studied by Raman Spectroscopy. *Phys. Rev. B* **2009**, *79*, 235429.
(33) Corio, P.; Santos, P. S.; Brar, V. W.; Samsonidze, G. G.; Chou, S. G.; Dresselhaus, M. S. Potential Dependent Surface Raman Spectroscopy of Single Wall Carbon Nanotube Films on Platinum Electrodes. *Chem. Phys. Lett.* **2003**, *370*, 675−682.
(34) Di Bella, S.; Lanza, G.; Fragala, I. L.; Marks, T. J. Electronic Structure, Molecular Geometry, and Bonding Energetics in Zerovalent Yttrium and Gadolinium Bis(arene) Sandwich Complexes. A Theoretical ab Initio Study. *Organometallics* **1996**, *15*, 3985−3989.
(35) Sarkar, S.; Zhang, H.; Huang, J.-W.; Wang, F.; Bekyarova, E.; Lau, C. N.; Haddon, R. C. Organometallic Hexahapto Functionalization of Single Layer Graphene as a Route to High Mobility Graphene Devices. *Adv. Mater.* **2013**, *25*, 1131−1136.
(36) Liu, X.; Wang, C.-Z.; Hupalo, M.; Lin, H.-Q.; Ho, K.-M.; Tringides, M. C. Metals on Graphene: Interactions, Growth Morphology, and Thermal Stability. *Crystals* **2013**, *3*, 79−111.
(37) Sarkar, S.; Niyogi, S.; Bekyarova, E.; Haddon, R. C. Organometallic Chemistry of Extended Periodic π-electron Systems: Hexahapto−Chromium Complexes of Graphene and Single-Walled Carbon Nanotubes. *Chem. Sci.* **2011**, *2*, 1326−1333.
(38) Wang, F.; Itkis, M. E.; Haddon, R. C. Enhanced Electromodulation of Infrared Transmittance in Semitransparent Films of Large Diameter Semiconducting Single-Walled Carbon Nanotubes. *Nano Lett.* **2010**, *10*, 937−942.

DOI: 10.1021/acsami.5b00942
ACS Appl. Mater. Interfaces 2015, 7, 28013−28018